Available online at www.sciencedirect.com
SCIENCE DIRECT®
Polymer 45 (2004) 3027–3036
polymer
www.elsevier.com/locate/polymer

Polymer intrusion into narrow pores at the interface between a poor solvent and adsorbing and non-adsorbing surfaces

G.F. Hermsen, M. Wessling, N.F.A. van der Vegt*

Membrane Technology Group, Faculty of Science and Technology, University of Twente, P.O. Box 217, 7500 AE Enschede, The Netherlands

Received 30 January 2004; received in revised form 27 February 2004; accepted 27 February 2004

Abstract

We report thermodynamic and conformational properties of collapsed polymer globules in a poor solvent close to adsorbing and non-adsorbing surfaces containing a cylindrical pore that is either smaller or larger than the coil size in bulk solution. Configurational Bias Monte Carlo simulations at infinite dilution were used for this purpose. We find that above the critical adsorption transition changing from good solvent to poor solvent conditions causes an increase of the partition coefficient due to cooperative monomer adsorption on the pore wall. Below the adsorption transition, the reverse effect is observed. The radius of gyration components as well as conformational (free) energies and entropies as a function of the chain centre of mass (CM) position along the pore axis reveal strong anomalies in the vicinity of the pore entrance. Below the adsorption transition, the dense globule in a poor solvent swells and deforms when penetrating the pore and recollapses once it is fully confined. Above the adsorption transition in solvents above and below the Θ-point, minima occur in the free energy at chain CM positions just in front of the pore entry causing a barrier upon pore penetration. Upon approaching the small pore from the bulk poor solvent region, the chain conformational entropy and energy run through a maximum below and above the adsorption transition.
© 2004 Elsevier Ltd. All rights reserved.

Keywords: Solvent quality; Adsorption; Membranes

1. Introduction

When the solvent quality of polymer solutions decreases, polymeric coils collapse into tight globules. This feature has great implications on polymer separation methods where porous interfaces are employed. In liquid chromatography and gel permeation chromatography (GPC) the solvent quality influences the migration and conformations of the polymers inside the matrix. In ultrafiltration of polymer solutions solvent quality also influences the separation e.g. a tightly packed polymer slightly larger than the membrane pore will not enter this pore whereas a flexible, swollen coil in a good solvent is able to permeate across it [1–3].

Polymer partitioning between solutions and micropores has been studied extensively both experimentally [4–6] and by computer simulations [6–11]. Most of these studies have dealt with the thermodynamic partitioning behaviour, which is determined by the properties of a fully confined polymer relative to those in the bulk polymer solution. When there is no attractive interaction between the polymer and the pore surface, the polymer chains are excluded from the pore according to their size relative to the pore size. In such a case, the partition coefficient K, defined as the polymer concentration in the pore relative to the polymer concentration in the bulk region, decreases as the molecular weight increases, which is the principle in GPC. It has been shown that when the pores at the interface are large compared to the polymer radius of gyration ($\lambda = R_g/R_p \ll 1$), the confinement energy and consequently the partition coefficient are not significantly affected by reducing the solvent quality [9]. At larger degrees of confinement ($\lambda \geq 1$), however, the confinement energy increases to very large values, resulting in negligible K values already before λ becomes unity [12].

When the polymers have attractive interactions with the surface of the pore and this attraction exceeds a certain threshold (the critical adsorption point), the polymers will adsorb on the surface of the pore. The longer the chain, the stronger the adsorption will be, therefore K will increase with the molecular weight. Reducing the solvent quality

* Corresponding author. Address: Max-Planck-Institute for Polymer Research, Ackermannweg 10, D55128 Mainz, Germany.
E-mail address: vdervegt@mpip-mainz.mpg.de (N.F.A. van der Vegt).

0032-3861/$ - see front matter © 2004 Elsevier Ltd. All rights reserved.
doi:10.1016/j.polymer.2004.02.063

then results in increasing partition coefficients where K rises to values larger than unity [11,13–15]. For infinitely long random walk chains the partition coefficient $K = 1$ at the adsorption transition but is slightly smaller for self avoiding walks (good solvent conditions) depending on the chain length M and the degree of confinement λ [15].

While many issues regarding the thermodynamic nature of polymer partitioning are well understood, much less attention has been devoted to polymer conformational changes and possible energetic (or entropic) barriers related to such changes upon penetrating pores smaller than the polymer size.

In this work we examine the conformational changes of collapsed polymer globules in poor solvent upon entering narrow cylindrical pores in adsorbing and non-adsorbing flat surfaces by means of Configurational Bias Monte Carlo simulations of a lattice chain model. In addition, detailed information on changes of the polymer's conformational entropy, energy, and free energy are presented. This paper extends upon our recent work reported on the same topic, which dealt with self avoiding chains partially confined at the entrance of a cylindrical pore in a flat surface [16,17].

The remainder of this paper consists of a description of the simulation method (section 2) after which the results are presented (section 3). The results section is split into two parts. First, we discuss the effect of changing the solvent quality on polymer conformational and thermodynamical properties at a porous interface under conditions that monomer-wall interactions are repulsive. In the second part, the same effects are discussed, but then monomer-wall interactions are attractive and stronger than the critical adsorption energy.

2. Simulation details

The simulation details are similar to those described in our previous work [16,17]. A lattice configurational bias sampling method [18] is used to carry out the simulations, combined with the bond fluctuation polymer model [19]. All simulated polymers are 50 monomers (M) long, each monomer taking up 8 grid points (a box) on a 3D simulation grid. Apart from their excluded volume interactions, the thermal (attractive) interactions between two grid points belonging to different non-bonded monomers, ϵ_{pp}, are varied between $0.00kT$ (good solvent), $0.2577kT$ (Θ solvent) and $0.30kT$ (poor solvent). When one or more of the grid points of the monomer-box is in contact with the wall, the monomer experiences an attractive interaction energy of 0 or $1.2kT$. The solvent Θ-point was found by computing R_g^2/M of isolated chains for $M = 20, 50, 100, 150$ and 200 and various ϵ_{pp} values and coincides with the ϵ_{pp} value where the curves intersect (not shown).

The critical adsorption point is determined using the method of Gong and Wang [15]. They used polymers end-grafted to a flat surface to calculate the polymer's excess chemical potential relative to its value when isolated in the bulk solvent and plotted this quantity as function of the monomer-wall interaction energy for various chain lengths. At the point where the graphs of the different chain lengths cross, the critical adsorption energy can be found. At this point the excess chemical potential becomes independent of the chain length [15]. We released the constraint of the end-graft and sampled conformations taking into account only the adsorbed chains in the calculation of the excess chemical potential. Polymer lengths of 30, 50, 70, and 100 monomers were used for this purpose. Fig. 1a, b and c shows the excess chemical potentials for polymers in a good solvent, a Θ-solvent, and a poor solvent ($\epsilon_{pp} = 0.30kT$), respectively. The critical adsorption point for a good solvent is situated at $\epsilon_{cr} = 0.96kT$. In Θ-solvents and in the poor solvent the critical adsorption points are $\epsilon_{cr} = 0.86kT$ and $\epsilon_{cr} = 0.77kT$, respectively.

The simulation box is set up by creating a flat surface with a straight cylindrical pore in the middle of the box. The length of the pore is large enough for the polymer to stretch out completely without finding its chain ends at opposite pore mouths (Fig. 2) [16]. The degrees of confinement, $\lambda = R_g/R_p$ (R_p being the pore radius), studied in this work are $\lambda = 0.5$ and $\lambda = 1.5$. If changes in solvent quality were made (and thus R_g changes), the pore radius was adjusted to satisfy these confinement degrees. In athermal solvents $R_g = 11.3$, under Θ conditions the R_g equals 8.7, and in poor solvent ($\epsilon_{pp} = 0.30$ kT)R_g equals 7.5. We note that at λ-values larger than 2.1 artefacts related to the underlying lattice appear in the excess chemical potential. Because all geometries including the cylindrical pore are modelled on a lattice, a scatter on the number of available adsorption sites as a function of the pore radius appears for $\lambda > 2.1$ due to irregularities of the cylinder. This causes artefacts in the energy inside the cylindrical pore. Conclusions drawn for λ values larger than 2.1 should therefore be taken with caution [17].

Chain conformational properties were calculated as a function of the polymer centre of mass z-position CM(z) (the direction along the pore axis) using the Rosenbluth weighting scheme: [20]

$$\langle \mathscr{A} \rangle_{\mathscr{R}} = \frac{\sum_{n=1}^{N} W(n)\mathscr{A}(n)}{\sum_{n=1}^{N} W(n)} \tag{1}$$

in which $\mathscr{A}$ is the configurational quantity of interest (e.g. the radius of gyration) and $W(n)$ denotes the Rosenbluth factor of conformation n. Chain conformations were generated segment by segment using a configurational bias favouring the energetic favourable monomer positions [18,20]. The z-position of the first chain segment was chosen randomly on the interval [−100,100] (Fig. 2). The x- and y-positions of the first monomer were taken at random within the available pore volume whenever $z < 0$ (inside the pore),

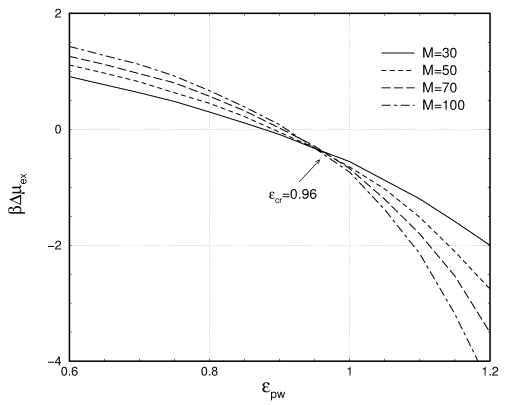

(a) $\epsilon_{cr} = 0.96kT$ at $\epsilon_{pp} = 0.0kT$

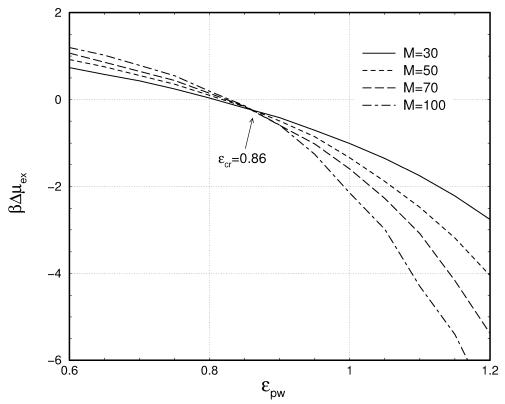

(b) $\epsilon_{cr} = 0.86kT$ at $\epsilon_{pp} = 0.2577kT$ (Θ-solvent)

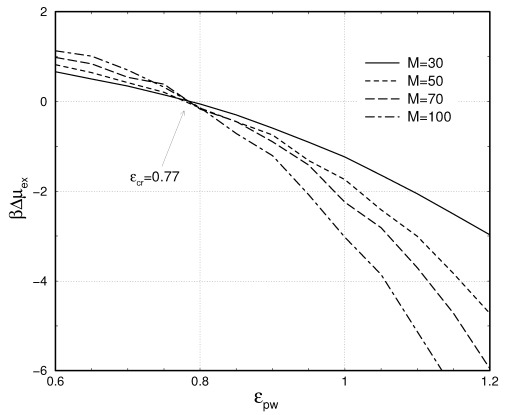

(c) $\epsilon_{cr} = 0.77kT$ at $\epsilon_{pp} = 0.30kT$

Fig. 1. Critical adsorption points in an athermal solvent ($\epsilon_{pp} = 0.0kT$), Θ-solvent ($\epsilon_{pp} = 0.2577kT$) and poor solvent ($\epsilon_{pp} = 0.30kT$). Critical adsorption points were determined by calculating chain excess chemical potentials near flat walls (Section 2).

whereas outside the pore they were randomly chosen within a radius of 2.5 R_g away from the pore axis. This choice allows the chains to adsorb on the flat surface facing the bulk solvent phase. The conformations used for statistical averaging were always those that had their centre of mass within a radius R_p from the pore axis. In this way, we obtain the conformational and thermodynamic properties of chains in front of the pore entry while still accounting for adsorption that may occur on the flat surface perpendicular to the pore axis. All averaged quantities (Eq. (1)) were accumulated as a function of the chain centre of mass z-position ($z \in [-100, 100]$). In total, 10^8 conformations were used for the ensemble average.

The excess chemical potential of a chain as a function of its centre of mass position along the pore axis was calculated from the probability to successfully insert it in the system, which in the Rosenbluth sampling scheme equates to the average Rosenbluth factor $\langle W \rangle$ obtained by averaging over all generated conformations. The excess chemical potential is obtained from $\beta\mu_{ex} = -\ln\langle W \rangle$ [21,22]. This quantity was calculated as function of the chain centre of mass z-position by updating a histogram at the appropriate entry (the bin value representing the centre of mass z-component) with the chain Rosenbluth factor W.

3. Results and discussion

3.1. Free energy profiles below and above the adsorption transition versus solvent quality

A profile of the excess chemical potential as function of the centre of mass position is plotted in Fig. 3a for various solvent qualities at degrees of confinement $\lambda \approx 1.5$. The monomer interaction with the wall is repulsive ($\epsilon_{pw} = 0.0kT$). Negative values for the centre of mass indicate that the polymer centre is inside the pore, positive values indicate that the polymer centre is inside the solvent. Inside the pore the excess chemical potential increases with decreasing quality of the solvent (ϵ_{pp} increases). This means that, under non-adsorbing conditions, the partition coefficient $K = \exp(-\beta\Delta\mu_{ex})$ decreases with decreasing solvent quality. The interface at $z = 0$ affects the chain chemical potential up to distances of at least 2 (bulk solvent) radii of gyration (20 grid points) in the pore or in the bulk solvent phase. Within this interface region strong changes in the chain conformation occur as will be discussed later on.

Fig. 3b shows the same profiles, but now the interaction of the monomers with the walls is strongly attractive i.e. $\epsilon_{pw} = 1.2kT$, well above the critical adsorption point in all solvents. Inside the pore, the order of the profiles is now reversed. The lower value of $\beta\Delta\mu_{ex}$ is obtained in a poor solvent, the higher value in a good solvent. Hence, at a fixed value of ϵ_{pw} above the adsorption transition, lowering the solvent quality leads to an increase of the partition coefficient. Note that decreasing the solvent quality causes a decrease of the critical adsorption energy ϵ_{cr} (Fig. 1). For $\epsilon_{pp} = 0.30$ kT the monomer-wall interaction energy ($\epsilon_{pw} = 1.2kT$) lies $0.45kT$ above ϵ_{cr}, for $\epsilon_{pp} = 0.0kT$ this value is $0.24kT$.

Increase of the partition coefficient achieved by reducing

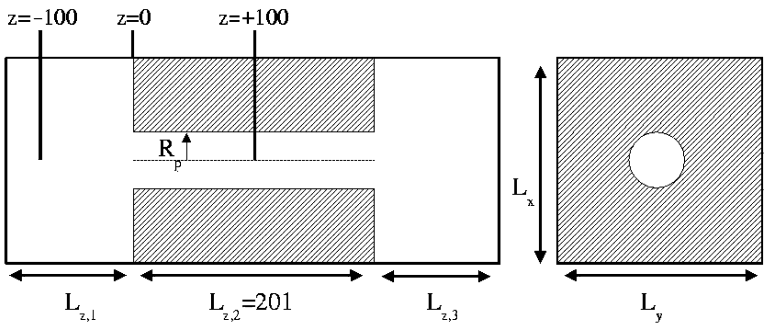

Fig. 2. Geometrical details of the simulation box. Cross sectional view (left) and top view (right).

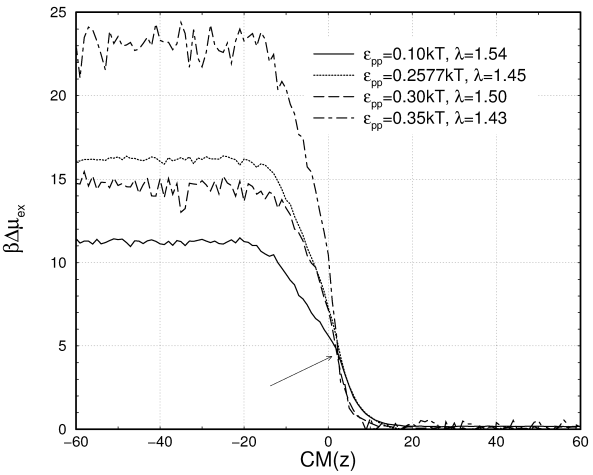

(a)

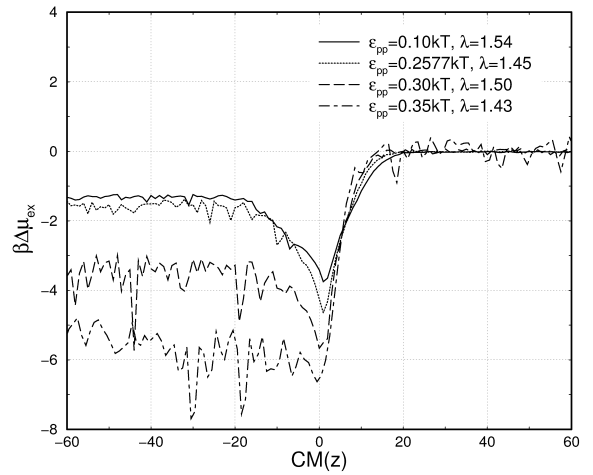

(b)

Fig. 3. $\beta\Delta\mu_{ex}$ profiles as function of the centre of mass CM(z) position at monomer-wall interaction energy $\epsilon_{pw} = 0.0kT$ (a) and $\epsilon_{pw} = 1.2kT$ (b). The degree of confinement is $\lambda \approx 1.5$ for various solvent qualities. Negative centre of mass values indicate that the polymer is inside the pore, at positive values the polymer is inside the solvent. The interface is positioned at CM(z) = 0. The R_g at $\epsilon_{pp} = 0.1$ and $0.35kT$ equal 10.8 and 5.7, respectively. Radii of gyration at the other conditions have been mentioned in Section 2.

the solvent quality can be attributed to cooperative adsorption of monomer units on the pore wall [23]. Whereas steric repulsions between monomers in a good solvent reduce the ability of a second monomer to adsorb close to the first, in a poor solvent mutual attractions between monomers promote the second monomer to adsorb close to the first.

Interestingly, free energy minima occur just in front of the pore entry at CM(z) = 0. While for CM(z) < 0 the adsorption energy favours a full chain confinement the entropic penalty associated with it causes the chain to preferably adsorb at the entry of the pore [17].

Below we present conformational changes, conformational energies and entropies at the pore entrance in a poor solvent. Details on what happens in athermal solvents have been reported elsewhere [16,17].

3.2. Partitioning in a poor solvent under non-adsorbing conditions

3.2.1. Conformational changes at the pore entry

In Fig. 4 snapshots are presented to illustrate the conformational changes occurring upon pore penetration ($\lambda = 1.5$). The accompanying changes in the radius of gyration components are shown in Fig. 5a. In bulk solvent (Fig. 4a) dense globules occur. In front of the pore entry (Fig. 4b), the globule slightly expands perpendicular to the pore axis to minimise the repulsion experienced from the surface. The polymer is slightly squeezed in the direction parallel to the pore axis and oriented into the perpendicular direction. The polymer has already penetrated the pore with one (Fig. 4c) or more (Fig. 4b) chain parts. Once the polymer penetrates the pore further (Fig. 4d) it loses its dense globular structure in order to make deformations possible to fit into the pore interior. As the chain penetrates the pore even further (Fig. 4e), the part of the chain inside the pore recollapses to experience the favourable intramolecular contacts again. In Fig. 5a this is revealed as a decrease of $R^2_{g,parallel}$ after passing through a maximum at CM(z) = −10. Once the chain has fully penetrated the pore (Fig. 4f) the R_g-components no longer change.

3.2.2. Conformational energy and entropy

Fig. 5b presents the chain excess chemical potential, β

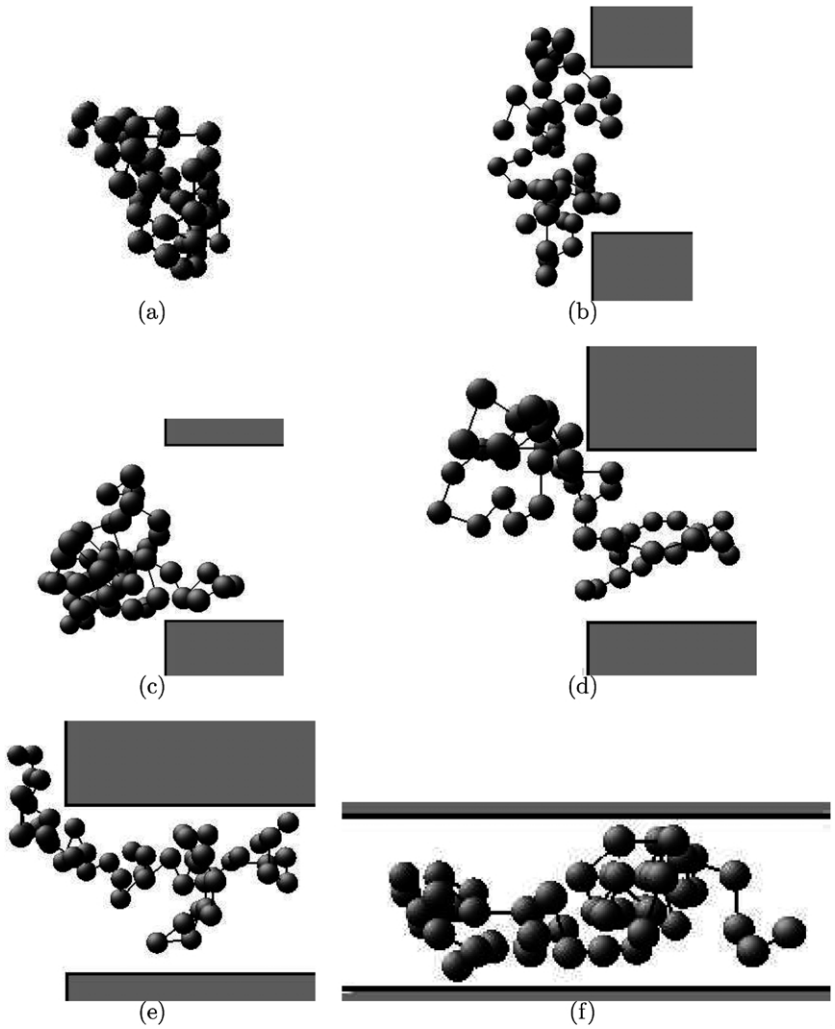

Fig. 4. Snapshots of polymer conformations under poor solvent conditions ($\epsilon_{pp} = 0.30kT$), degree of confinement $\lambda = 1.5$ and repulsive walls ($\epsilon_{pw} = 0.0kT$).

$\Delta\mu_{ex}$, and its entropic ($\Delta S_{ex}/k$) and energetic ($\beta\Delta U_{ex}$) components. When the chain CM approaches the pore entry, both the conformational entropy and intramolecular energy start to decrease at CM(z) = 12 (approximately 1.5 bulk radius of gyration in front of the pore entry). Note that in Fig. 5a the $R^2_{g,parallel}$ starts to decrease as well. To avoid repulsions experienced from the flat surface the globule adopts a compressed conformation with its main axis oriented perpendicular to the pore axis. Due to this chain compaction, the number of intramolecular contacts between the monomers increases and $\beta\Delta U_{ex}$ decreases. This decrease is compensated by the conformational entropy that decreases too, but stronger. As a net result, the chain excess chemical potential, $\beta\Delta\mu_{ex} = \beta\Delta U_{ex} - \Delta S_{ex}/k$, shows no extremum at the pore entry and increases monotonically with decreasing CM(z).

As soon as the chain centre of mass enters the pore, the conformational entropy and energy increase, reach a maximum, and next decrease toward a constant value. At the maximum, chain conformations resemble those depicted in Fig. 4e. At full chain confinement (Fig. 4f), both the energy and entropy have decreased below their respective values in the bulk solvent phase. The confinement value $\lambda = 1.5$ causes a compression of the globule leading to a reduction of its internal energy and conformational entropy.

Degrees of confinement smaller than unity, i.e. $\lambda = 0.5$, show different behaviour of the energetic and conformational properties. In Fig. 6b the maxima in $\beta\Delta U_{ex}$ and $\Delta S_{ex}/k$ that were present in Fig. 5b appear also here, but now these are clearly smaller and are shifted towards CM(z) values closer to the pore entrance. Despite the pore radius being twice as large as the bulk radius of gyration, the energetic and entropic components decrease to values well below the respective values in the bulk solvent indicating deformations taking place at the interface although to a much lesser extent than at $\lambda = 1.5$. The radius of gyration components shown in Fig. 6a no longer reveal strong anomalies: the weak minimum in front of the interface and the weak maximum inside the pore for the parallel R^2_g component remains visible, both shifted towards slightly larger CM(z) values.

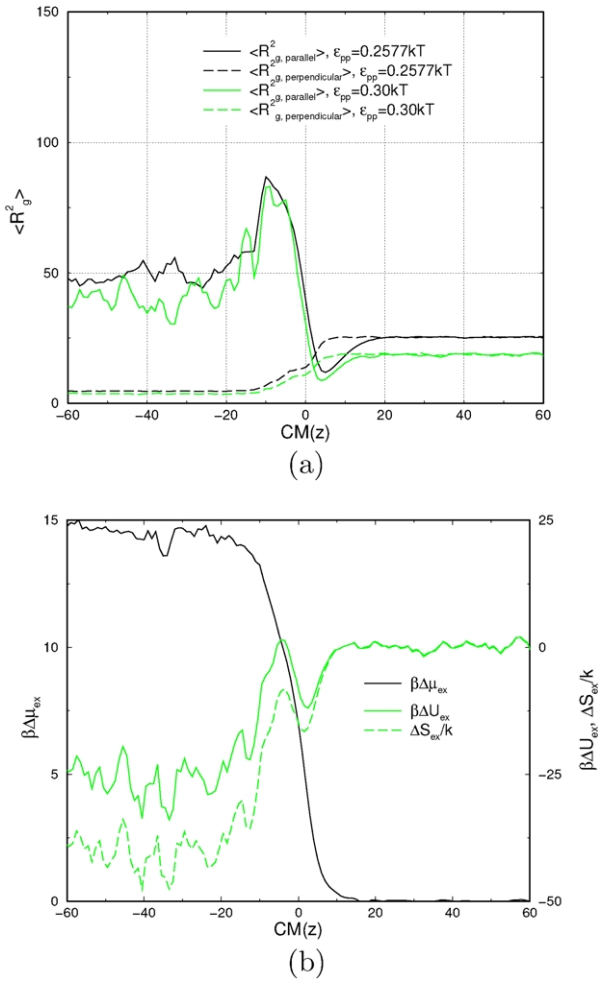

Fig. 5. Radius of gyration components of polymers as function of the centre of mass at varying solvent qualities ϵ_{pp} (a) and their energetic properties in a poor solvent ($\epsilon_{pp} = 0.30kT$) (b), $\lambda = 1.5$ near repulsive walls ($\epsilon_{pw} = 0.0kT$).

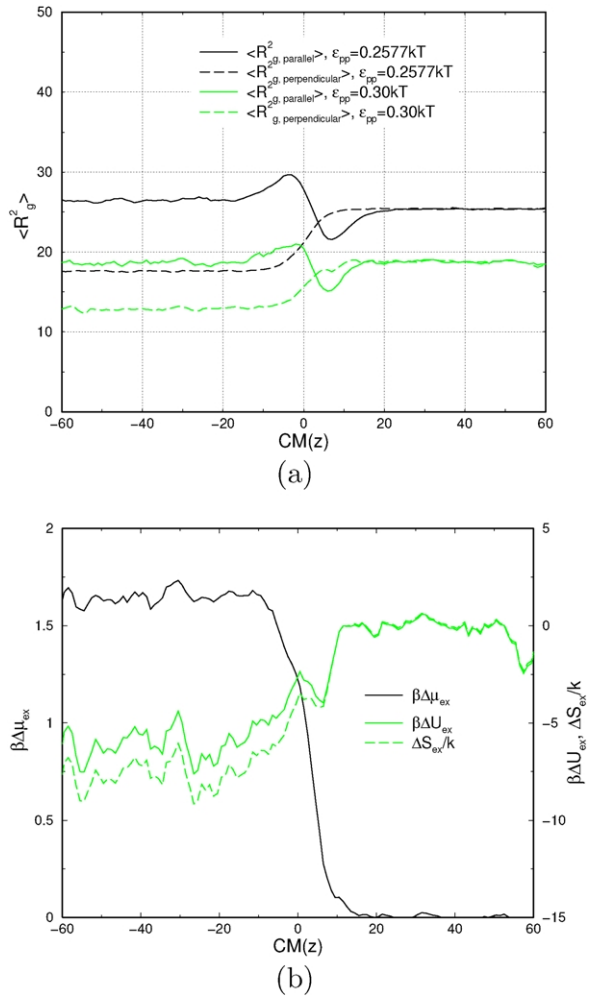

Fig. 6. Radius of gyration components of polymers as function of the centre of mass position at varying solvent qualities ϵ_{pp} (a) and energetic properties in a poor solvent ($\epsilon_{pp} = 0.30kT$) (b), $\lambda = 0.5$ and repulsive walls ($\epsilon_{pw} = 0.0kT$).

3.3. Partitioning in poor solvent under strong adsorption conditions

3.3.1. Conformational changes at the pore entry

Whereas below the adsorption transition the pore penetration is much determined by the chain's attempt to avoid the surface, now adsorption effects strongly determine the observed mechanism. Fig. 7 illustrates what happens in a poor solvent with a confinement degree $\lambda = 1.5$ and a monomer wall energy $\epsilon_{pw} = 1.2kT \gg \epsilon_{cr}$. Fig. 8a shows the accompanying changes of $R^2_{g,perpendicular}$ and $R^2_{g,parallel}$. At distances within 1–3 bulk radii of gyration from the surface (CM(z) < 20) the dense globular structure is partly sacrificed in order to adsorb onto the surface (Fig. 7b). Although, it involves disrupting attractive intramolecular monomer contacts there is a considerable payback in terms of the adsorption energy and conformational entropy as will be shown below. Fig. 8a shows that $R^2_{g,parallel}$ may increase by as much as 75% giving rise to a strong maximum in this quantity of approximately one bulk radius of gyration in front of the pore entrance. This feature occurs in an athermal solvent as well, however, opposite to what we find here for $\epsilon_{pp} = 0.30kT$, it reduces the conformational entropy [17]. When the polymer approaches the surface closer, $R^2_{g,parallel}$ decreases below the bulk solvent value due to strong adsorption of the chain onto the surface (Fig. 7c and d).

The adsorbed chain either fully covers the pore entry while having small parts of the chain adsorbed in the pore ('drawing pins' [17], Fig. 7c) or adsorbs on a smaller part of the outer surface while having a larger number of repeat units adsorbed on the pore wall. The chain eventually enters the pore (Fig. 7e) by desorbing monomers from the outer surface and adsorbing them inside. At this point, $R^2_{g,parallel}$ runs through a second maximum because the longest coil axis initially oriented perpendicular to the pore axis (Fig. 7c and d) needs to reorient. Moreover, the conformations in Fig. 7c and d have the lowest free energy (see Figs. 3b and 8b), hence monomers try to remain at the interface while the chain centre of mass moves further into the pore (Fig. 7e). The minimum in free energy corresponds to a maximum in

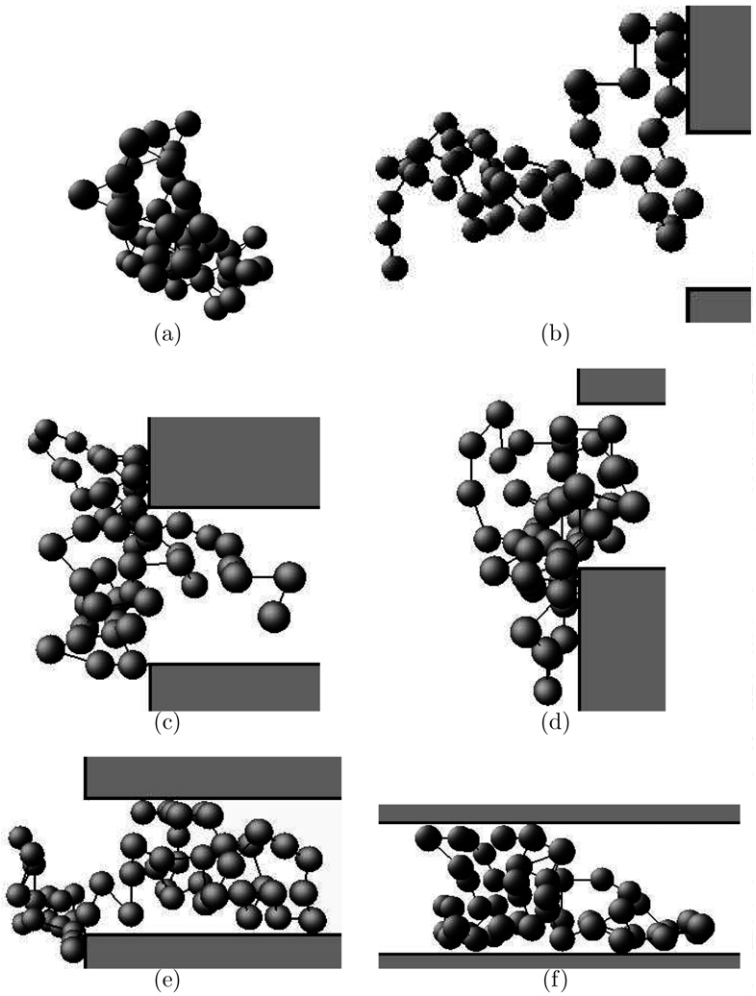

Fig. 7. Snapshots of polymer conformations under poor solvent conditions ($\epsilon_{pp} = 0.30kT$), degree of confinement $\lambda = 1.5$ and attractive walls with an interaction potential above the critical adsorption energy ($\epsilon_{pw} = 1.2kT$).

the monomer density versus CM(z) (not shown) [16]. Only when CM(z) < -20 (almost 3 solvent bulk radii of gyration), $R^2_{g,parallel}$ becomes constant.

3.3.2. Conformational energy and entropy

Fig. 8b shows the energy and entropy changes associated with the pore penetration process in Fig. 7. The energetic component of $\beta\Delta\mu_{ex}$ has been split into two contributions. The first, $\beta\Delta U_{ex}$, measures energy changes due to variation in the number of intramolecular monomer contacts. The second contribution, $\beta\Delta E_{ex}$, measures the energy of adsorption. At 1 bulk radius of gyration in front of the pore entrance, $\beta\Delta U_{ex}$ and $\Delta S_{ex}/k$ reach a maximum. At this distance, the chain tries to adsorb on to the surface (Fig. 7b) at the expense of disrupting the attractive monomer contacts within the globule. The increase of $\beta\Delta U_{ex}$ is compensated by a slightly larger negative contribution of $\beta\Delta E_{ex}$ while the conformational entropy assumes a value equal to the entropy of the globule in the bulk poor solvent. At CM distances closer to the surface, corresponding to the snapshots in Fig. 7c and d, intramolecular contacts are restored and $\beta\Delta U_{ex}$ decreases. In addition, the conformational entropy decreases. The adsorption energy, $\beta\Delta E_{ex}$, now decreases faster because at these close distances between the surface and the chain centre of mass, monomers can more and more readily adsorb.

Note that the monomer-monomer energy ($\epsilon_{pp} = 0.30kT$) in the example of Fig. 7 matches closely with the monomer-wall energy $\epsilon_{pw} = 1.2kT$ (at maximum contact, two non-bounded monomers experience an attractive energy of $1.2kT$). Solvent quality (as determined by ϵ_{pp}) affects the energetic and entropic features correspondingly to the adsorption phenomenon in Fig. 7b. In Θ-solvent and athermal (good) solvents, chain adsorption is driven by the adsorption energy while a decrease of the conformational entropy, unlike in the situation here, opposes it [17]. The conformational changes in Θ and good solvents [17] are stronger as can be seen in Fig. 8a for $R^2_{g,parallel}$ in Θ-solvent.

At CM(z) $= 0$, the chain chemical potential, $\beta\Delta\mu_{ex}$, is at a minimum. Note that at this point $\beta\Delta E_{ex}$ and $\beta\Delta U_{ex}$ are not. The minimum in $\beta\Delta\mu_{ex}$ may thus be regarded as a compromise between the attempt of the polymer to

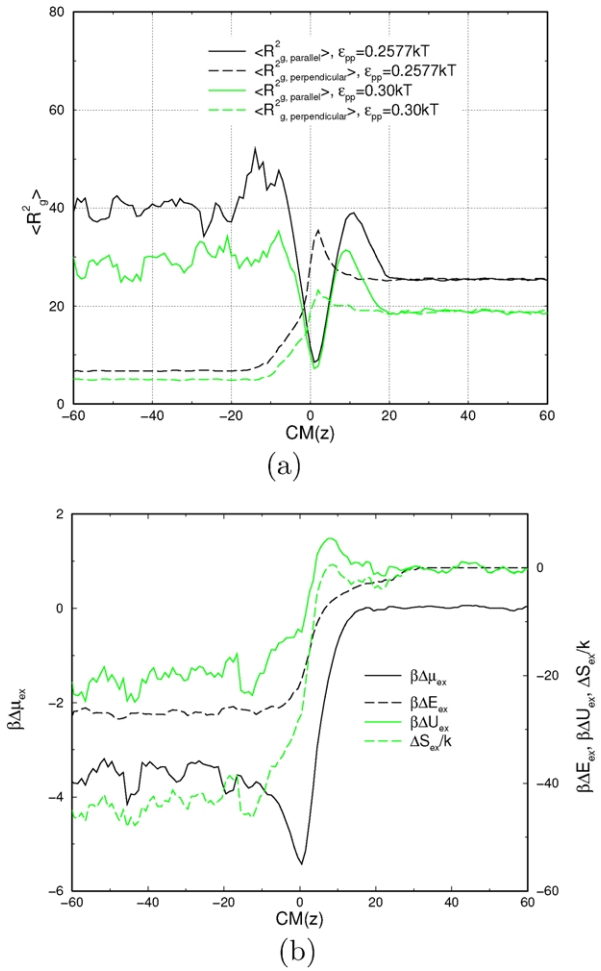

Fig. 8. Polymer radius of gyration components as function of the centre of mass position at varying solvent qualities (ϵ_{pp}) (a) and energetic polymer properties in a poor solvent ($\epsilon_{pp} = 0.30kT$) (b), $\lambda = 1.5$ and with strongly attractive walls ($\epsilon_{pw} = 1.2kT$).

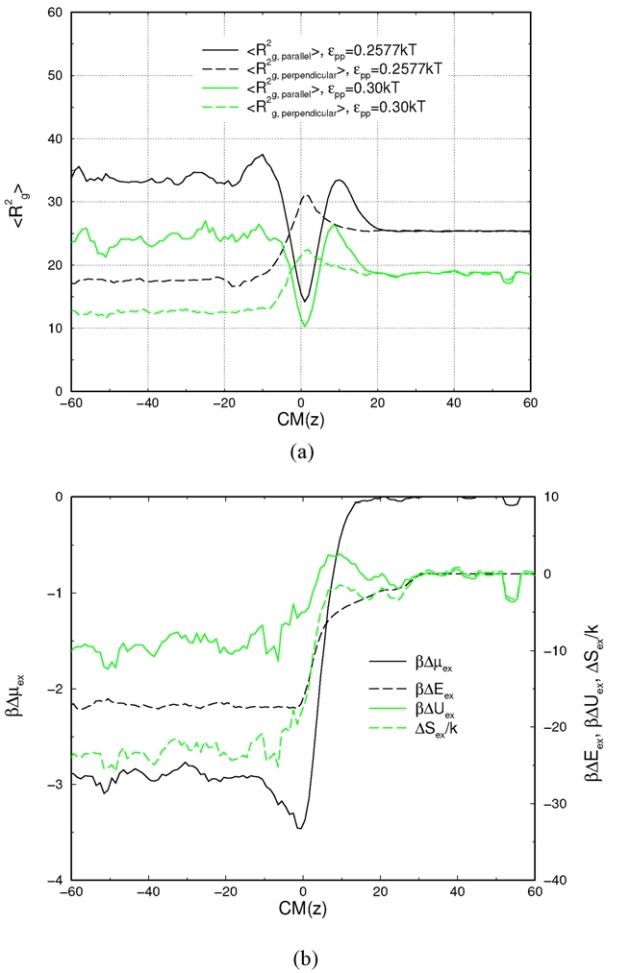

Fig. 9. Polymer radius of gyration components at varying solvent qualities ϵ_{pp} (a) and energetic properties in a poor solvent ($\epsilon_{pp} = 0.30kT$) (b), $\lambda = 0.5$ and with strongly attractive walls ($\epsilon_{pw} = 1.2kT$).

minimise its energy while maintaining conformation flexibility (entropy). Because, in the pore interior $\beta\Delta\mu_{ex} < 0$, the partition coefficient is larger than unity ($K \approx 30$). This example therefore demonstrates the existence of an entropic barrier in front of a strongly adsorbing cylindrical confinement.

Fig. 9a and b shows the thermodynamic quantities and radii of gyration components versus the chain centre of mass position at a smaller degree of confinement ($\lambda = 0.5$). Noteworthy, all features present in Fig. 8a and b ($\lambda = 1.5$) are retained. All characteristic conformations shown in Fig. 7 for $\lambda = 1.5$ occur at $\lambda = 0.5$ as well although deformation of the globule occurs to a lesser extent. A weak minimum of $\beta\Delta\mu_{ex}$ is still present at the pore entry despite the much smaller confinement degree.

3.3.3. Loops and trains

To gain better insight in the nature of chain adsorption in solvents of different quality, we have examined the properties of adsorbed trains and the loops that connect them. The shape of the graphs for the number of trains n_t as function of the polymer centre of mass in poor solvent at $\lambda = 1.5$ is very similar to the situation for a good solvent (Fig. 10). Upon approaching the surface the number of trains increases equally fast independent of the solvent quality until 2 grid points in front of the surface where n_t for $\epsilon_{pp} = 0.0$ kT has a light kink after which it starts to level off to a constant value ($n_t \approx 8$) at around CM(z) $= -20$ (inside the pore).

The number of trains for the poor solvent has a higher value inside the pore and reaches its constant value ($n_t \approx 10$) at CM(z) $= -15$, slightly closer to the interface. For $\epsilon_{pp} = 0.30kT$ and $\lambda = 0.5$ the behaviour at the interface is different. The graph shows a sharper kink than the other graphs due to weaker deformation of the chain upon entering the pore and does not change any further once inside the pore.

Fig. 11a shows the average train length of adsorbed polymers for $\lambda = 1.5$ in a good solvent and a poor solvent and for $\lambda = 0.5$ in poor solvent. Fig. 11b shows the average loop length for the same situations. From about 1 bulk radius of gyration in front of the pore entry to far inside the

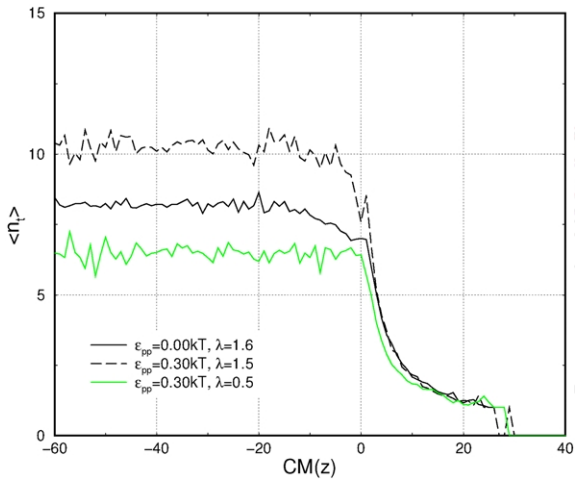

Fig. 10. Average number of trains per adsorbed polymer as function of centre of mass position in a poor ($\epsilon_{pp} = 0.30kT$) and a good solvent ($\epsilon_{pp} = 0.0kT$) for $\lambda = 1.5$ and 0.5 with strongly attractive walls ($\epsilon_{pw} = 1.2kT$).

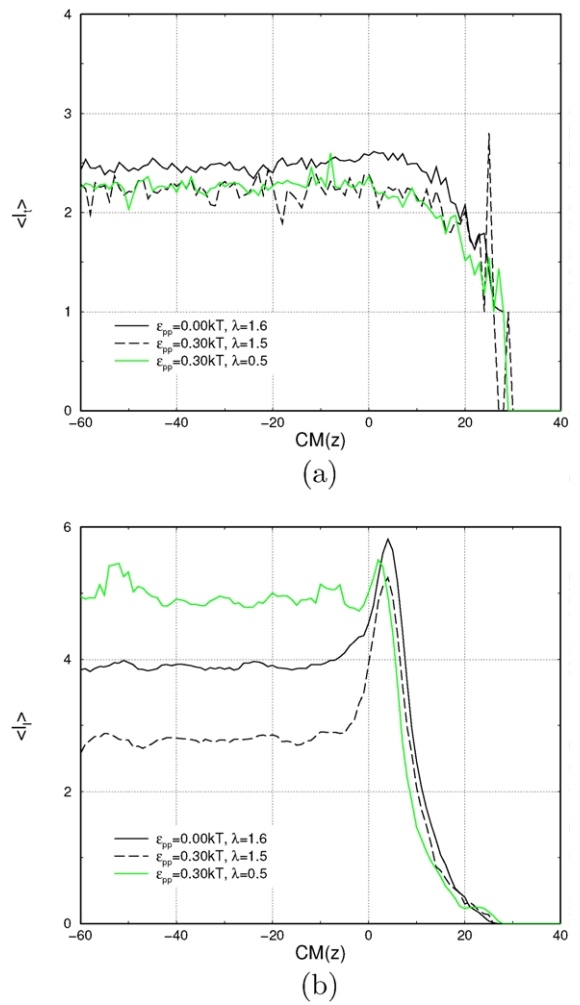

Fig. 11. Train lengths (a) and loop lengths (b) of adsorbed polymers as function of centre of mass position at poor ($\epsilon_{pp} = 0.30kT$) and good solvent conditions ($\epsilon_{pp} = 0.0kT$), $\lambda = 1.5$ and 0.5 with strongly attractive walls ($\epsilon_{pw} = 1.2kT$).

pore the average train lengths remain constant. The lengths of the trains for both solvents are comparable where the trains for athermal chains are slightly larger. Lowering the degree of confinement in the poor solvent does not significantly affect the average train length. The number of trains shown in Fig. 10 indicates that although the length of the trains is slightly shorter in poor solvent, the number of trains is significantly larger resulting in a net larger amount of adsorbed monomers in the poor solvent due to the co-operative adsorption effect discussed above.

The loop lengths in Fig. 11b show a large peak for both solvents at $\lambda = 1.5$ in front of the interface. This is due to polymers partly adsorbed on the outer surface at $z = 0$ and on the inside pore wall. These polymers will have large loops connecting trains inside the pore to the trains adsorbed on the surface. Polymers bridging across the pore entrance contribute significantly to the large loop length in front of the surface as well. At $\lambda = 0.5$, the peak at the pore entrance is very weak as bridging across the pore entry becomes less probable.

Lowering the solvent quality gives rise to shorter loops inside the pore. The peak in the loop length in front of the surface is only slightly smaller than the peak for the good solvent. The geometry of the pore has a large effect on the height of the loop length peak in front of the surface.

4. Summary and conclusions

Polymer penetration into narrow pores on a flat surface requires significant conformational changes at the interface. In this paper, we have examined how collapsed polymer chains (globules) in a poor solvent enter small pores on non-adsorbing and adsorbing surfaces. The degrees of confinement λ, defined as the unperturbed polymer radius of gyration relative to the pore radius, were chosen $\lambda = 1.5$ and $\lambda = 0.5$. Using the Rosenbluth sampling method, computer simulations were performed with the bond fluctuation model to compute chain conformational properties, chain excess chemical potentials, as well as conformational entropies and energies as a function of the distance between the chain centre of mass and the pore entrance.

On non-adsorbing surfaces, polymer intrusion occurs through two major conformational changes. Within one bulk radius of gyration in front of the pore entrance, the approaching globule is compressed in the direction normal to the surface. Once the chain centre of mass approaches the pore entrance the globule is distorted and elongated parallel to the pore axis at both values of λ. The R_g-component parallel to the pore axis runs through a maximum upon intrusion and levels off once the chain is completely confined. The over-extension upon intrusion causes a maximum in the chain conformational entropy and energy.

On adsorbing surfaces the intruding globule is not as significantly distorted along the direction of the pore axis. Instead, significant conformational changes occur prior to

intrusion. At one bulk radius of gyration in front of the pore entrance, the chain globular nature is lost due to the chain's attempt to adsorb. This causes chain elongation along the direction normal to the interface. Next, the chain adsorbs at the interface covering the pore entrance. This situation corresponds with a minimum of the chain excess chemical potential as a function of the chain centre of mass position along the pore axis. At this position the chain R_g-component parallel to the pore axis is at a minimum and chain segments only marginally explore the pore entry. The conformations here are very similar to the conformations found in a good solvent at attractive energies above the critical adsorption energy, although more tightly packed [17]. The polymer intrusion process proceeds by desorbing segments from the interface and adsorbing them on the inner pore surface causing the parallel R_g-component to increase. This process is favoured by the energetic part of the chain excess chemical potential but strongly opposed by the conformational entropy part for both degrees of confinement $\lambda = 1.5$ and $\lambda = 0.5$ and causes a free energy barrier for pore penetration.

References

[1] Baker RW, Strathmann H. Ultrafiltration of macromolecular solutions with high-flux membranes. J Appl Polym Sci 1970;14:1197.

[2] Beerlage MAM, Heijnen ML, Mulder MHV, Smolders CA, Strathmann H. Non-aquous retention measurements: ultrafiltration behaviour of polystyrene solutions and colloidal silver particles. J Membr Sci 1996;113:259.

[3] Beerlage MAM, Peeters JMM, Nolten JAM, Mulder MHV, Strathmann H. Hindered diffusion of flexible polymers through polyimide ultrafiltration membranes. Appl Polym Sci 2000;75:1180.

[4] Gorbunov AA, Ya Solovyova L, Skvortsov AM. General mechanism of the chromatography of macromolecules: experimental test of the universal nature of adsorption effects. Polymer 1998;39:697.

[5] Skvortsov AM, Gorbunov AA, Berek D, Trathnigg B. Liquid chromatography of macromolecules at the critical adsorption point: behaviour of a polymer chain inside pores. Polymer 1998;39:423.

[6] White JA, Deen WM. Equilibrium partitioning of flexible macromolecules in fibrous membranes and gels. Macromolecules 2000;33:8504.

[7] Davidson MG, Suter UW, Deen WM. Equilibrium partitioning of flexible macromolecules between bulk solution and cylindrical pores. Macromolecules 1987;20:1141.

[8] Deen WM. Hindered transport of large molecules in liquid-filled pores. AIChE J 1987;33:1409.

[9] Cifra P, Bleha T, Romanov A. Monte-Carlo calculations of equilibrium partitioning of flexible chains into pores. Polymer 1988; 29:1664.

[10] Lin NP, Deen WM. Effects of long-ranged polymer–pore interactions on the partitioning of linear polymers. Macromolecules 1990;23: 2947.

[11] Cifra P, Bleha T. Partition coefficients and the free energy of confinement from simulations of nonideal polymer systems. Macromolecules 2001;34:605.

[12] Bleha T, Mlýnek J, Berek D. Concentration dependence of chain dimensions and its role in gel chromatography. Polymer 1980;21: 799.

[13] Gorbunov AA, Skvortsov AM. Statistical properties of confined macromolecules. Adv Colloid Interf Sci 1995;62:31.

[14] Cifra P, Bleha T. Steric exclusion/adsorption compensation in partitioning of polymers into micropores in good solvents. Polymer 2000;41:1003.

[15] Gong Y, Wang Y. Partitioning of polymers into pores near the critical adsorption point. Macromolecules 2002;35:7492.

[16] Hermsen GF, de Geeter BA, van der Vegt NFA, Wessling M. Monte Carlo simulation of partially confined polymers. Macromolecules 2002;35:5267.

[17] Hermsen GF, van der Vegt NFA, Wessling M. Monte Carlo simulations of polymer adsorption at the entrance of cylindrical pores in flat adsorbing surfaces. Soft Mater 2003;1:295.

[18] Frenkel D, Smit B. Understanding molecular simulation: from algorithms to applications, 2nd ed. New York: Academic Press; 2002.

[19] Carmesin I, Kremer K. The Bond fluctuation method: a new effective algorithm for the dynamics of polymers in all spatial dimensions. Macromolecules 1988;21:2819.

[20] Rosenbluth MN, Rosenbluth AW. Monte Carlo simulations of the average extension of molecular chains. J Chem Phys 1955;23:356.

[21] Harris J, Rice SA. A lattice model of a supported monolayer for amphiphilic molecules: Monte Carlo simulations. J Chem Phys 1988; 88:1298.

[22] Siepmann JI. A method for the direct calculation of chemical potentials for dense chain systems. Mol Phys 1990;70:1145.

[23] Scheutjens JMHM, Fleer GJ. Statistical theory of the adsorption of interacting chain molecules. 1. Partition function, segment distribution, and adsorption isotherms. J Phys Chem 1979;83:1619.